GEOLOGICAL INTERPRETATION OF 2D GRAVITY MODELING IN TULUNG SELAPAN AREA AND SURROUNDINGS, SOUTH SUMATRA BASIN

INTERPRETASI GEOLOGI DARI PEMODELAN GAYABERAT 2D DI DAERAH TULUNG SELAPAN DAN SEKITARNYA, CEKUNGAN SUMATRA SELATAN

Eddy Mirnanda[1*], Vera Sarah Simatupang[2], Harkins Prabowo[3]

[1] Research Center for Geological Resource, BRIN, Jl. Sangkuriang, Kel. Dago, Kec. Coblong, Bandung 40135

[2] Geophysical Engineering, Institut Teknologi Sumatera (ITERA), Jl. Terusan Ryacudu, Kel. Way Hui, Kec. Jati Agung, Lampung Selatan 35365

[3] Marine Geological Institute – Geological Agency, Jl. Dr. Djunjunan No. 236, Kel. Husen Sastranegara, Kec. Cicendo, Bandung 40174

*Corresponding author: eddy006@brin.go.id

(Received 12 December 2022; in revised from 14 December 2022; accepted 25 January 2023)

DOI : http://dx.doi.org/10.32693/bomg.37.2.2022.796

ABSTRACT: The South Sumatra Basin is a prolific oil and gas basin. The Tulung Selapan area, which is to the east and part of the South Sumatra Basin, is considered to have hydrocarbon potential. Several sub-basins, including the South Palembang and the North Palembang sub-basins, exist in the region. One of the geophysical methods for determining the presence of sedimentary sub-basins, structural patterns, and bedrock is the gravity method. The purpose of this study is to determine the structural pattern and interpret the subsurface geological model of the Tulung Selapan area using 2D modeling. The complete Bouguer anomaly (CBA) reveals circular and relatively northwest-southeast trending patterns, ranging from +33 mGal to +62 mGal. 2D gravity forward modeling results in eight successive rock layers. From top to bottom, the uppermost layer is swamp sediment with a mass density of 2.1 g/cm^3, followed successively by the sedimentary rocks of the Kasai Formation (2.28 g/cm^3), the Muara Enim Formation (2.32 g/cm^3), the Air Benakat Formation (2.39 g/cm^3), the Gumai Formation (2.3 g/cm^3), the Baturaja Formation (2.48 g/cm^3), and lastly a layer with a density of 2.7 g/cm^3, which represents the bedrock. Due to the limited depth of 2800 m in 2D forward modeling, it is unable to identify the source and reservoir rocks. The seal rock (caprock) is interpreted to be shale from the Gumai Formation at an average depth of 1.53 km. Based on Second Vertical Derivative (SVD) analysis, 2D modeling identifies the presence of geological structures with normal faults.

Keywords: Gravity, Second Vertical Derivative (SVD), 2D Modeling, Tulung Selapan, South Sumatra Basin

***ABSTRAK**: Cekungan Sumatra Selatan adalah salah satu cekungan sedimen yang telah terbukti menghasilkan minyak dan gas bumi. Daerah Tulung Selapan merupakan bagian dari cekungan Sumatra Selatan yang berada di sebelah timur dan diduga memiliki potensi hidrokarbon yang ditandai adanya beberapa sub-cekungan seperti sub-cekungan Palembang Selatan, dan sub-cekungan Palembang Utara. Metode geofisika yang dapat digunakan untuk mengetahui keberadaan sub-cekungan sedimen, pola struktur, dan batuan dasar pada penelitian ini adalah metode gayaberat. Tujuan dari penelitian ini adalah untuk mengetahui pola struktur dan menginterpretasi geologi bawah permukaan daerah Tulung Selapan berdasarkan pemodelan 2D. Anomali Bouguer lengkap (ABL) daerah Tulung Selapan berkisar antara +33 mGal hingga +62 mGal berpola melingkar serta berarah relatif barat laut-tenggara. Hasil pemodelan gayaberat menghasilkan delapan lapisan batuan berturut-turut dari atas ke bawah adalah endapan rawa dengan densitas 2.1 gr/cm^3 yang merupakan lapisan paling atas, kemudian di bawahnya adalah batuan sedimen Formasi Kasai dengan rapat massa (2.28 gr/cm^3), Formasi Muara Enim (2.32 gr/cm^3), Formasi Air Benakat (2.39 gr/cm^3), Formasi Gumai (2.3 gr/cm^3), Formasi Baturaja (2.48 gr/cm^3), dan 2.7 gr/cm^{3}mewakili batuan dasar (*basement*). Karena pemodelan 2D terbatas sampai kedalaman 2800 m, batuan* *induk dan reservoir tidak dapat teridentifikasi. Batuan penutup (*seal*) diduga merupakan Formasi Gumai (2.3 gr/cm^3) yang berada pada kedalaman rata-rata 1.53 km berupa serpih. Hasil pemodelan 2D menunjukkan adanya struktur patahan turun yang teridentifikasi berdasarkan analisis* Second Vertical Derivative *(SVD).*

Kata Kunci: *Gayaberat,* Second Vertical Derivative *(SVD), Pemodelan 2D, Tulung Selapan, Cekungan Sumatra Selatan.*

INTRODUCTION

Petroleum exploration in Indonesia has been going on since the 19th century. Over the past decade, oil production has decreased. In 2009, production reached 346 million barrels (949k bpd); then it fell to 283 million barrels (778k bpd) in 2018. This decline in production levels is due to the age of the main oil-producing wells, which are generally old, and the fact that only a few new oil-producing wells have been established (Sekretariat DEN, 2019).

Due to the subduction of the Indian-Australian Plate beneath the Sunda Shelf microplate, a series of back-arc basins, primarily onshore, were created aligned northwest-southeast along Sumatra Island, with some extending to the east coast waters off Sumatra. The basins were initially formed by three consecutive major tectonic phases of extension, relative quiescence, and compression (Suhendan, 1984). Among these basins is the South Sumatra Basin, which is Tertiary structural and composed of Tertiary sedimentary rocks overlying pre-Tertiary metamorphic and igneous rocks unconformably (de Coster, 1974). The South Sumatra Basin is divided into four sub-basins, namely Jambi, Central Palembang, North Palembang, and South Palembang (Panggabean & Santy, 2012). The research area is located in the Tulung Selapan area, between three sub-basins: the North, Central, and South Palembang sub-basins (Setiadi et al., 2010).

Bishop (2000) argued that the history of the South Sumatra basin's structure encompasses three mega-sequences that control the geological structures: syn-rift (40-29 Ma), post rift (29-5 Ma), and syn-orogenic and inversion (5 Ma – present). Such structures created because of those tectonic events are faults, horst, and graben, as well as uplift or anticlinorium. The initial step taken in hydrocarbon exploration is describing conditions and identifying subsurface structures to minimize the risk of failure during exploration.

A study of geophysical approaches is needed to identify subsurface geological structures. One of the geophysical methods that can be used to determine subsurface conditions is the gravity method. This method is based on differences in the densities of the rocks beneath the surface (e.g., Setiadi et al., 2014) and usually used for preliminary surveys in oil and gas or mining exploration. The basic principle of the gravity method uses variations in the earth's gravitational field as a result of lateral density contrast (Rosid & Siregar, 2017). The gravity anomaly measured on the surface is a combination of long-wavelength (regional) anomaly, short-wavelength (residual) anomaly, and noise (Karunianto, 2017).

Bouguer anomalies are defined to see more detailed geological structure patterns. To distinguish influences between regional anomalies originating from deeper rocks and residual anomalies deriving from shallower rocks, the anomalies need to be filtered. Bedrock is often the deeper rock with a higher density that can be found from the crust to the Moho. High densities influence the values of Bouguer anomalies that are measured on the surface. Therefore, it is necessary to separate between regional and residual anomalies. The filtering method used in this study is moving average filter.

Modeling the gravity anomaly data is expected to provide information related to basin structure based on the distribution of rock density. By matching calculation and observation data with trial-and-error process using 2D forward modeling, basin structure can be described (Grandis, 2009). Identification of structural boundaries is carried out using the Second Vertical Derivative (SVD) method (Rosid & Siregar, 2017). The combined results of gravity data analysis and geological information are then used to interpret the geological conditions of the study area.

Based on the results of spectral analysis in the South Sumatra Basin, there are two discontinuity planes in this area, namely the bedrock at a depth of about 3.05 km and the Mohorovicic discontinuity (the Moho) at a depth of about 15.98 km (Setiadi et al., 2010). As a result of the 2D modeling, an overview of the subsurface geological information of the Tulung Selapan and its surrounding area has been defined. The resolution of its geological information is used to assist in determining and locating faults in subsurface geological models based on their gravity data.

The South Sumatra Basin and Central Sumatra Basin are large basins located on Sumatra Island and bounded by the Tigapuluh Mountains (Tarsis, 2001). The South Sumatra Basin itself is a back-arc basin (Panggabean & Santy, 2012), as seen in the map of the South Sumatra Basin with tectonic appearances (Figure 1). The basin is bordered by the Barisan Mountains, Jambi and the Bangka Basin to the west; the Thirty and Twelve Mountains to the north; the Sunda Shelf (Java Sea) to the east; and the Lampung Highs to the south. Specifically, the Tulung Selapan area is located between two sub-basins, namely the North and South Palembang sub-basins.

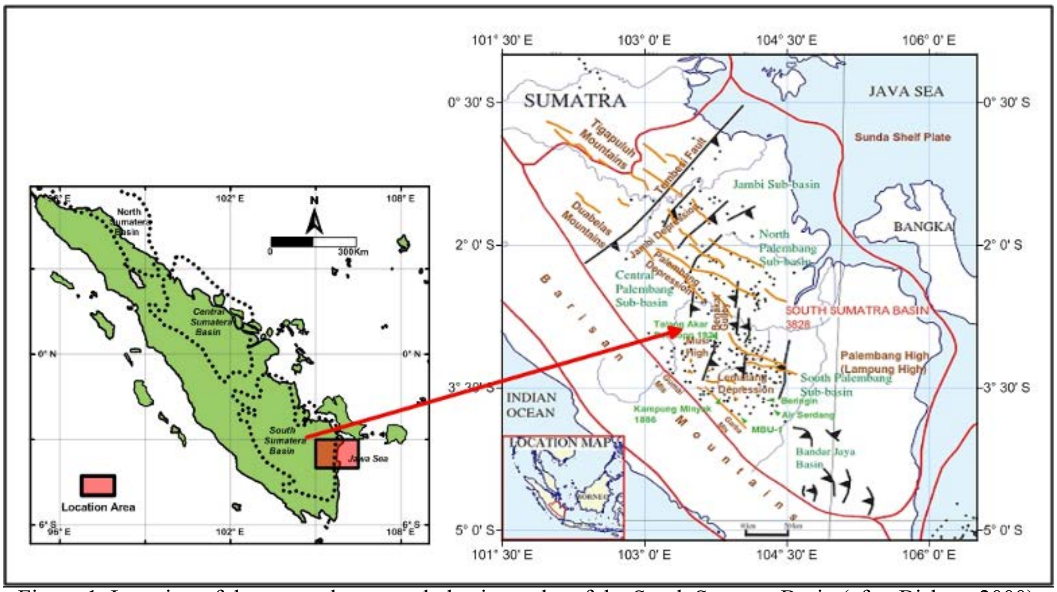

Figure 1. Location of the research area and physiography of the South Sumatra Basin (after Bishop, 2000)

The study area is part of the Tulung Selapan Quadrangle (Mangga et al., 1993) and covers around 13,200 km^2 (Figure 1). The Tulung Selapan area is situated on the east coast of the southern part of Sumatra Island, which is geographically located between 3˚- 4˚S and 105˚-106.5˚E. The quadrangle is bounded by the quadrangles of Pangkalpinang to the north; Menggala to the south; Lahat to the west; and the Java Sea to the east.

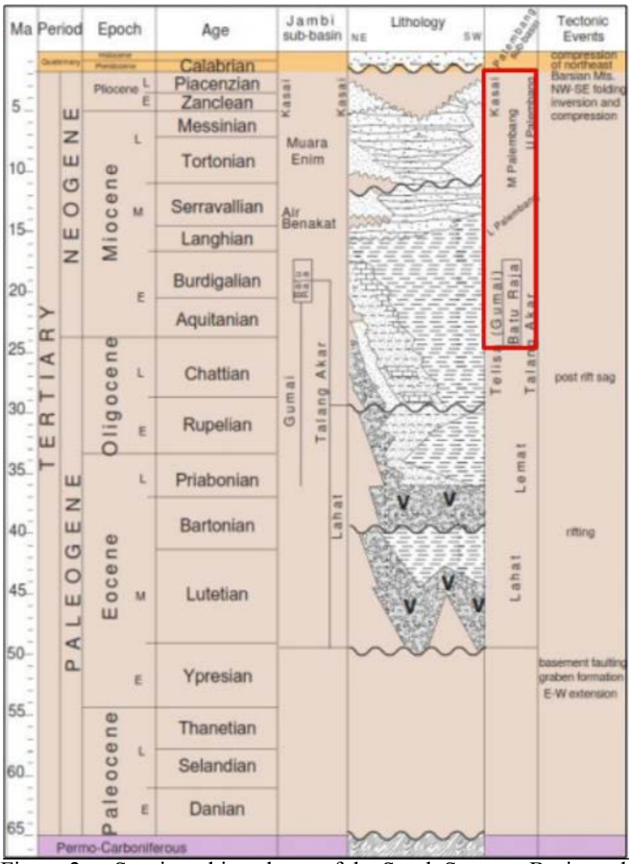

Figure 2. Stratigraphic column of the South Sumatra Basin, red box marked the stratigraphy of the study area. (Courteney et al., 1990; de Coster, 1974; Sudarmono et al., 1997; Hutchison, 1996; Sosrowidjojo et al., 1994).

The Tulung Selapan area is within the South Sumatra Basin, where the bedrock was formed during the pre-Tertiary period and overlain unconformably by Tertiary sediments. The stratigraphy of the South Sumatra Basin basically happened in one major cycle of deposition that can be broken down into two depositional phases, i.e., the transgression phase at the beginning and the regression phase at the end of the cycle. Respectively, the transgression phase occurred during Middle Oligocene to Miocene, covering the Telisa Group. Deposited successively from old to young, the Telisa Group consists of the Lahat Formation (deposited in a fluviatile-lacustrine environment), the Talang Akar Formation (transitional deposition), the Baturaja Formation (shallow marine depositional environment), and the Telisa/Gumai Formation (deep marine depositional environment). The regression phase took place in the Middle Miocene to Pliocene with a property change in the successive formation deposition, covering the Palembang Group. From old to young, the group comprises the Air Benakat Formation (shallow marine depositional environment), the Muara Enim Formation (transitional deposition), and the Kasai Formation (deposited in a fluviatile-terrestrial environment). These sedimentary deposits were then overlain unconformably by Quaternary deposits, as shown in Figure 2 (Wahyudin & Subekti, 1999).

Referring to the geological map of the Tulung Selapan Quadrangle (Figure 3), the stratigraphy of the study area consists of alluvium (Qa), swamp deposits (Qs), coastal deposits (Qc), and granite (Jgr/Gr), which was formed as intrusive igneous rocks during the Quaternary. The Muara Enim Formation (Tmpm), the Kasai Formation

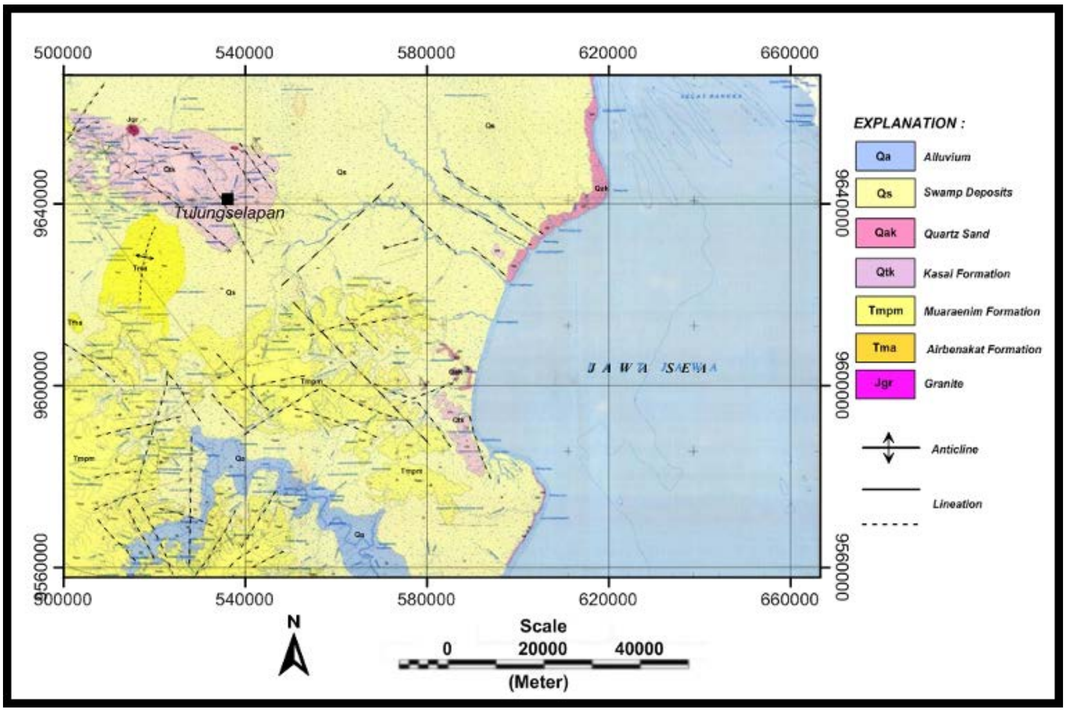

Figure 3. Geological map of Tulung Selapan Quadrangle, South Sumatra (after Mangga et al., 1993)

(QTk), the Gumai Formation (Tmg), the Air Benakat Formation (Tma), and the Baturaja Formation (Tmb) were deposited during the Tertiary (Mangga et al., 1993).

The oldest rock in the Tulung Selapan area is the Baturaja Formation of the Early Miocene, and conformably overlaid the top of the Talang Akar Formation. Successively overlying the Baturaja Formation is the Gumai Formation, which is composed of shale, sandstone, siltstone, and limestone. The formation was followed conformably by the deposition of the Air Benakat Formation that comprises shale, in which intercalations of limestone and calcareous sandstone are discovered, and interbedding of claystone/siltstone. The overlying formations above the Air Benakat Formation are the Muara Enim and the Kasai Formations. The Muara Enim Formation conformably overlaid the Air Benakat Formation and is composed of tuffaceous claystone, clay, and sandstone, with carbonaceous siltstone and lignite spotted at the top. The Kasai Formation has an unconformity boundary with the Air Benakat. The Kasai Formation consists of tuff and tuffaceous sandstones, as well as grayish sandstones with iron oxide gravel. The Kasai formation also overlaid the Muara Enim Formation unconformably (Mangga et al., 1993).

METHODOLOGY

Gravity data were obtained in the year 2000 in field activities with the Geological Research and Development Center (GRDC), now Center for Geological Survey (CGS) – Geological Agency, using the LaCoste & Romberg gravimeter instruments models of G.240 and G.816. These measurements were collected from as many as 118 measurement points, which were spread randomly at intervals of 1.5 km up to 10 km.

The data acquired from the gravity measurements in the field are in the form of Complete Bouguer Anomaly (CBA) values. Several corrections, which include: drift, tidal, and topographic conditions (height, terrain, latitude, and Bouguer corrections), were applied to the measurement results. A spectral analysis, a step carried out to estimate the depth of a discontinuity field as a cause of gravity anomaly, was performed to distinguish the CBA values into residual and regional anomalies. The optimum window width is used to exemplify the differences between regional and residual anomalies in the research area using the moving average method.

Bouguer anomaly is a disturbance in the earth's gravitational field as a result of lateral density contrast, and can also be caused by the presence of anomalous objects located below the surface at both shallow depths (residual anomalies) and deep depths (regional anomalies). The Complete Bouguer Anomaly (CBA) is obtained from equation (1) as follows:

$$CBA = Gobs - Gn - FAC - BC + TC \quad (1)$$

(Blakely, 1996)

where:

CBA = Complete Bouguer Anomaly (mGal)
$Gobs$ = Observation gravity acceleration (mGal)
Gn = Gravity acceleration after corrected for latitude (mGal)
FAC = Free Air Correction (mGal)
BC = Bouguer Correction (mGal)
TC = Terrain Correction (mGal)

The next process is the Second Vertical Derivative (SVD) method, which is used to identify the boundaries of the structure in a research location. Identification of structural boundaries is conducted by analyzing the existence of zero-value contours located between high-value and low-value contours with an orientation following the dominance of the fault structure direction from a geological perspective. This study uses the Elkins filter operator (Elkins, 1951).

Defining the subsurface structures is fulfilled using modeling. A residual anomaly map resulting from moving average filtering is needed as a basis for the modeling, as well as the need for a map of the research area equipped with the geological information and a map of the residual of their estimated density values in the depths.

Quantitative interpretation is carried out to determine a model of subsurface geological conditions by analyzing each trajectory model, processed by the 2D forward modeling (Setiadi et al., 2010). Geosoft Oasis Montaj software is used to execute the modeling process. In general, the complete research flowchart can be seen in Figure 4.

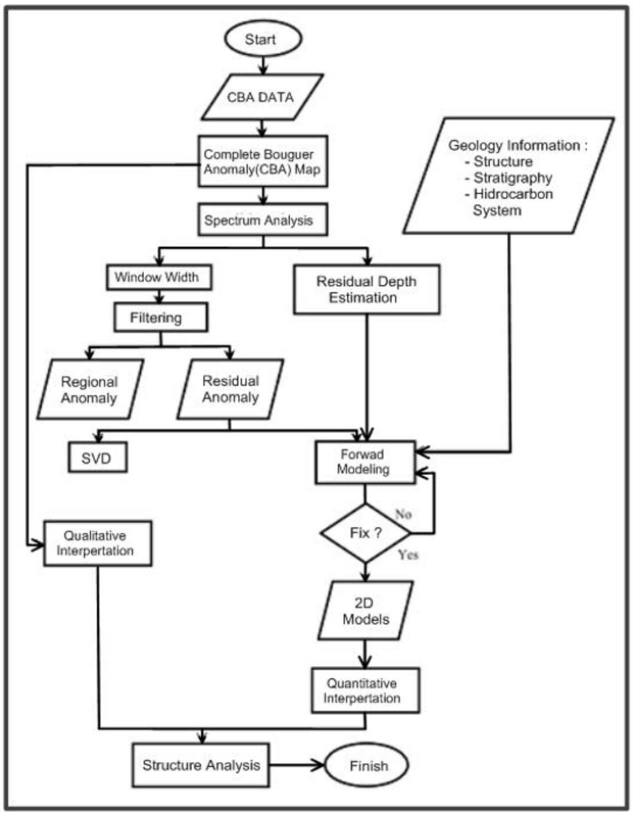

Figure 4. Flowchart of the research analyses

RESULTS AND DISCUSSION

Bouguer anomalies are composed of regional and residual anomalies. Regional anomalies are due to deep anomalies, characterized by low frequency and long-wavelength. On the other hand, shallow anomalies with high frequency and short-wavelength are the cause of residual anomalies.

Figure 5 reveals an anomalous pattern of Bouguer anomalies with a relative trend in the northwest-southeast direction and similarly circular patterns in some places. The map shows Complete Bouguer Anomaly (CBA) values of the Tulung Selapan area that range from +33 mGal to +62 mGal, in consideration of the criteria of low anomalies valued from +33 mGal (dark blue) to +41 mGal (light blue), moderate anomalies valued from +42 mGal (light blue) to +47 mGal (orange), and high anomalies valued from +48 mGal (red) to +62 mGal (pink).

High anomalies represent rocks with high density, while low anomalies reflect rocks with low density. In the northwest, there is a high anomaly distribution that is precisely located in the Bukit Batu area. An intrusion rock of granite from the Holocene period is found in this area and exposed to the surface. In the northeast, low anomaly patterns are disclosed precisely in the Rawang Lebong Hitam and Rawang Sungai Duabelas areas. This cluster of low anomalies is interpreted as thin deposits consisting of swamp deposits and alluvium that covered the area.

Spectral analysis is a step applied to estimate the depth of a discontinuity plane caused by the gravity anomalies. The optimum window width works as a filter to separate regional anomalies from residual anomalies in an observation area. Initially, the stage begins with gridding on several trajectories, of which gravity anomalies from the CBA are considered to be included. In this study, the gridding stage was carried out on eight designated trajectories, lined along the locations of measurement points that appeared dominant across the area. This is done to avoid gridding on the interpolated CBA values (Figure 5).

After trajectory gridding, the data is then converted using the Fourier transform, done with numerical software, to generate real and imaginary values for each measurement distance taken from the gridding. The imaginary values are then calculated using equation (2) to get the values of k (wave number) and *ln A* (natural logarithm of the amplitude).

$$ln\, A = (z_0 - z')|k| \quad \ldots \ldots \ldots \ldots \ldots \ldots (2)$$

(Blakely, 1996)

These two parameters will then be plotted, with k being on the x-axis and *ln A* being on the y-axis. Derived from the k and *ln A* plots, regional, residual, and noise anomalies will be classified based on the slope (gradient) of each anomaly trend. Two examples of plotting eight trajectory lines are graphs shown in Figure 6, namely the B-B' and F-F' trajectories. Based on the graph, the values of m (gradient) and C (constant) are obtained for each trajectory.

The intersection between the gradients of regional and residual anomalies is labeled *kc*, named for the boundary of the continuity plane in between. The values of *m* (gradient) and *C* (constant) contained in each gradient of the anomaly trend are processed to obtain regional and

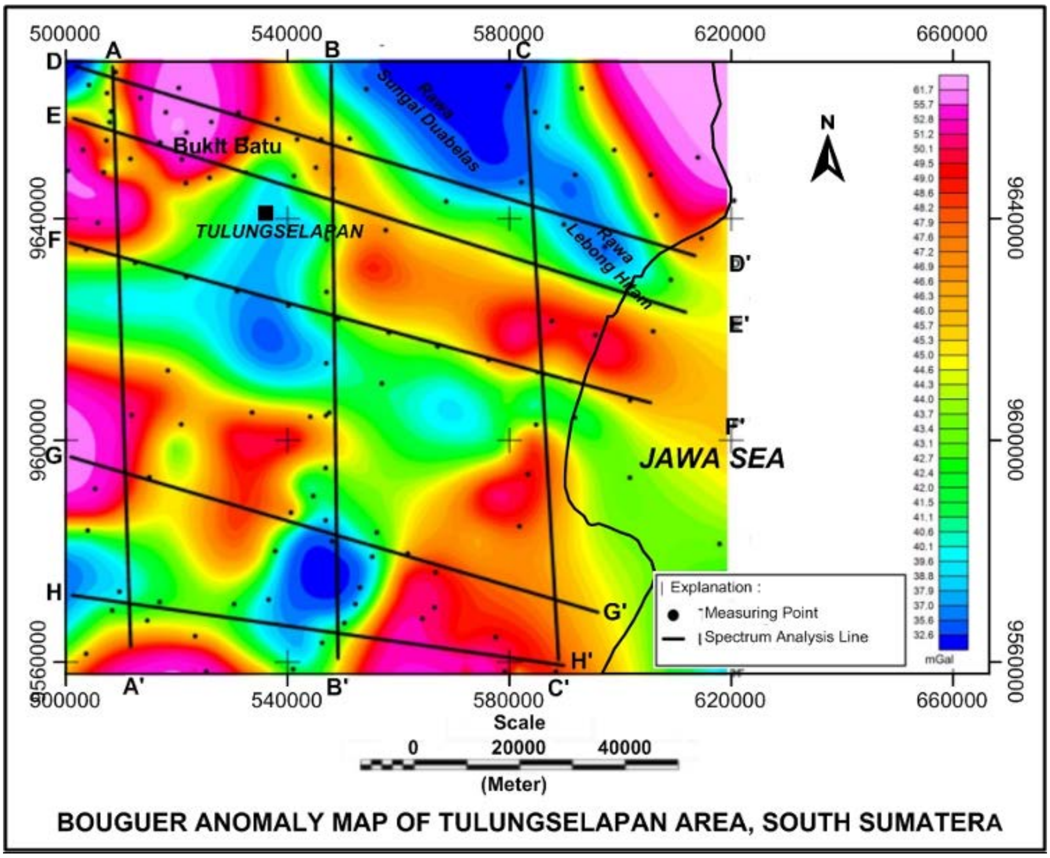

Figure 5. Bouguer anomaly map of Tulung Selapan area with eight designated trajectories drawn based on locations of most populated measurement points

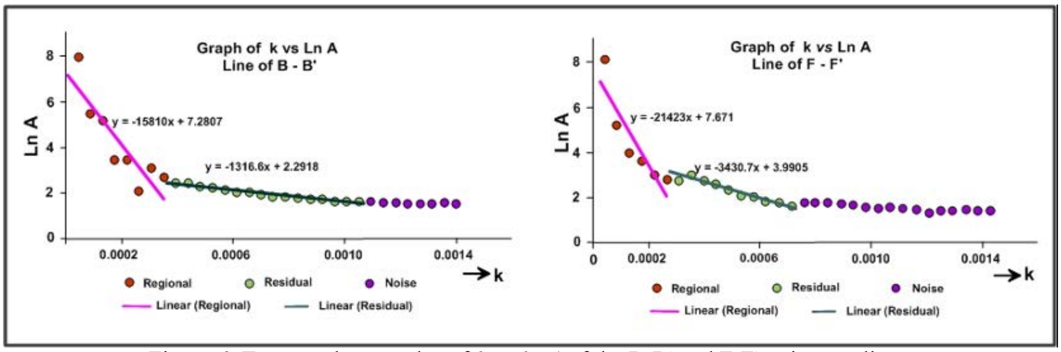

Figure 6. Two graph examples of ***k*** vs ***ln A*** of the B-B' and F-F' trajectory lines

residual depths. An optimum window width is applied in order to separate regional and residual anomalies (Table 1).

Each track has a different regional anomaly depth value, residual value and window width. Therefore, the values for these three variables on each track must be averaged. The window width value is calculated following equation (3).

$$\Delta g_r = \frac{\Delta g_{(B1)} + \Delta g_{(B2)} + \cdots + \Delta g_{(B21)}}{21} \quad \text{........(3)}$$

(Blakely, 1996)

After averaging, the regional anomaly depth is about 17.5 km, the residual depth is about 2 km, and the optimum window width is 20.5342 (≈ 21). To separate regional and residual anomalies from Bouguer gravity data, the window width value of ~21 customized for this area is inputted in the moving average filtering process. The result of the process is regional anomalies.

Based on the regional anomaly map below (Figure 7), the distribution of regional anomalies in the Tulung Selapan area ranges from +36 mGal to +58 mGal, in consideration under the criteria for low anomalies varying from +36 mGal (dark blue) to +42 mGal (light blue), moderate anomalies valued between +43 mGal (green) and +45 mGal (orange), and high anomalies ranging from +46 mGal (red) to +58 mGal (pink).

The residual anomaly is generated by subtracting the regional anomaly from the Complete Bouguer Anomaly (CBA). Residual anomalies generally represent areas of a discontinuity plane at shallow depths. The value distribution of residual anomalies in the Tulung Selapan area ranges from -4.3 mGal to +4.4 mGal (Figure 8), with

Table 1. Anomaly depth and window width of each trajectory

Line of	m1 (Regional)	m2 (Residual)	k	λ	N
A - A'	-17225	-1810	0.00035626	17636.67	16.0333
B - B'	-15810	-1316.6	0.00030075	20891.674	18.9924
C - C'	-21734	-3626.9	0.00030163	20830.559	18.9369
D - D'	-14838	-1485.1	0.00030823	20385.049	18.5319
E - E'	-15056	-1542.9	0.00026448	23757.047	21.5973
F - F'	-21423	-3430.7	0.00020456	30715.651	27.9233
G - G'	-15692	-1491.9	0.00030745	20436.543	18.5787
H - H'	-18570	-1581.9	0.00024122	26047.972	23.68
Average Depth	-17543.5	-2035.75	Average Window Width		20.5342

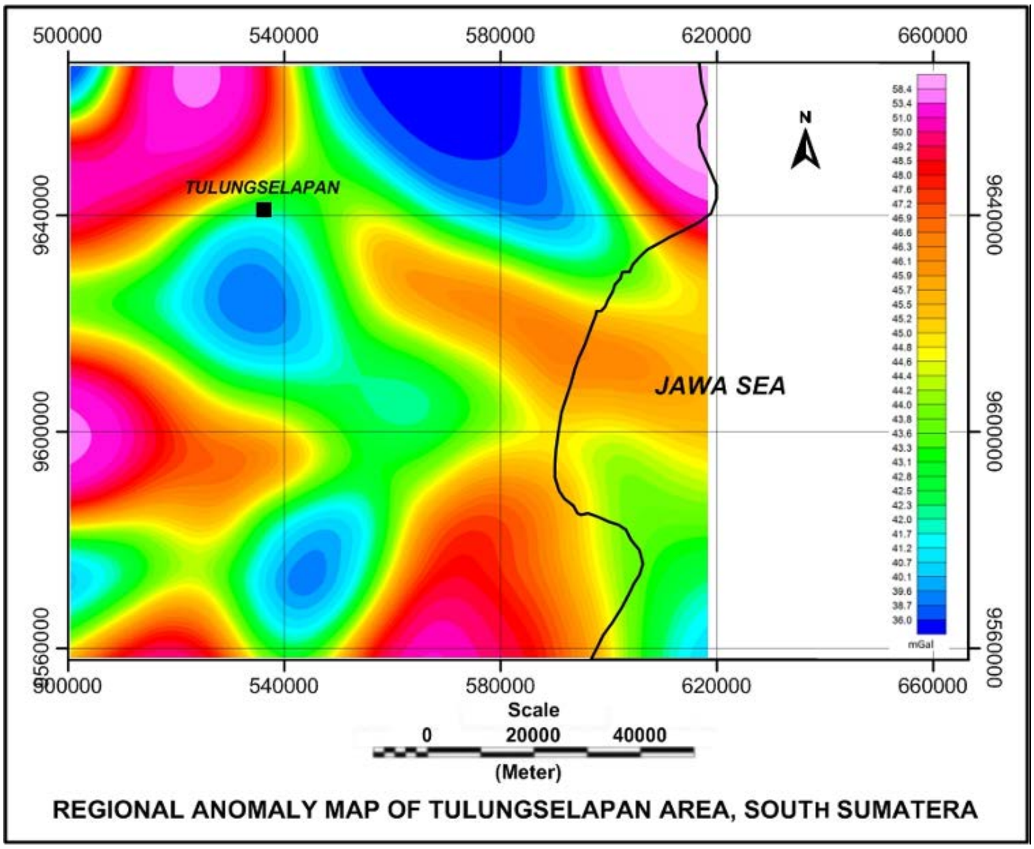

Figure 7. Regional anomaly map of Tulung Selapan area, showing the patterns of anomalies with northwest-southeast directions and sporadic circular patterns

regard to the classification of low anomalies ranging from -4.3 mGal (dark blue) to -1.8 mGal (light blue), moderate anomalies spanning from -1.8 mGal (green) to +0.2 mGal (orange), and high anomalies varying from +0.2 mGal (red) to +4.4 mGal (pink).

Reckoning the residual anomaly map in Figure 8, in the northwest, high anomalies that lengthen to the southeast are assumed to be several granite intrusions flowing upward to the surface and exposed as outcrops. Other high anomalies in the southern part are interpreted as the Muara Enim Formation, whereas high anomalies in the southwest extending to the west represent the Air Benakat Formation. In the northeast, high anomalies mark the presence of the Kasai Formation. As for low anomalies with circular patterns, they generally represent small sub-basins, composed of swamp and alluvium deposits.

In the SVD method, the boundary of the geological structure is bound to a value of zero, or close to zero. Referring to Reynolds (1997), fault type can be identified based on the following criteria:

$|SVD|min < SVD|max$ is the normal fault;
$|SVD|min > SVD|max$ is the thrust fault;
and $|SVD|min = SVD|max$ is the strike fault.

The SVD method has the characteristic of a high-pass filter, through which only high frequency signals can pass. Residual anomalies typically have high-frequency patterns that reveal shallow geological structures. The

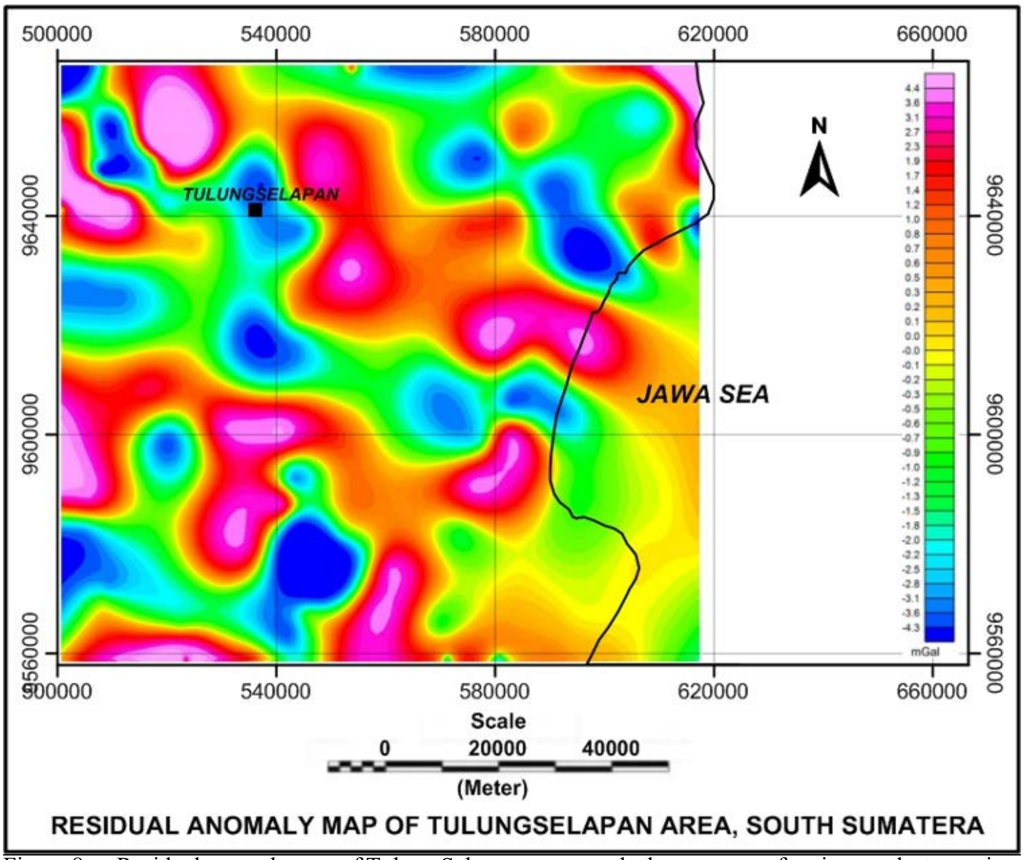

Figure 8. Residual anomaly map of Tulung Selapan area reveals the presence of various rocks types, i.e., sedimentary and igneous rocks

method in this study was performed using the SVD 2D Elkins operator and calculated through Laplace's equation. Based on the SVD map (Figure 9), three types of fault structures can be classified: faults identified geologically (white lines), faults predicted by SVD (blue lines), and faults confirmed by SVD (red lines on the map).

Based on the analysis of the SVD map for the Tulung Selapan area, high-value (red-pink) and moderate (green-orange) anomalies dominate evenly in the center and on the edges of the study area. The resulting values of the anomaly range from -0.51 mGal to +0.50 mGal, with categories of low anomaly values that vary from -0.51 mGal (dark blue) to -0.08 mGal (light blue), moderate anomaly values that range from -0.08 mGal (green) to +0.02 mGal (orange), and high anomaly values that have a range from +0.02 mGal (red) to +0.50 mGal (pink). According to Figures 11, 12, and 13, the SVD anomaly value, which is 0 and marked by the yellow color between the high and low anomalies, is interpreted as the presence of fault structures beneath the surface.

2D forward modeling was developed to interpret subsurface geological conditions in the Tulung Selapan area by creating trajectories in a southwest-northeast direction that passes through the North Palembang and South Palembang sub-basins. Considering the residual anomalies, modeling is carried out on three trajectory lines, namely A-A’, B-B’, and C-C' (Figure 10).

The South Palembang and the North Palembang sub-basins are traversed by the A-A' trajectory over a distance of 94 km (see Figure 10). Trajectory A-A' passes the South Palembang Sub-basin between 0 and 28.6 km. The residual anomaly values range from -4.0 mGal to -0.33 mGal. The response of the gravity anomaly is relatively sloping. Based on the geological map, no faults have been found in this sub-basin, but it is suspected that an anticline with a height of up to 20 m is exposed on the surface. The sedimentary rocks composing the anticline outcrop are oriented west to east and originated from the Air Benakat Formation. At a distance of 28.6 to 94 km, the trajectory passes the North Palembang sub-basin with a residual anomaly value of -0.33 mGal to +2.31 mGal. Here, the response of the gravity anomaly decreases and then increases. Based on the geological map, five normal faults were identified in this sub-basin (Figure 11).

The trajectory A-A’ modeling results in six formations of sedimentary rocks and possibly basement/bedrock. Sequentially, the rock formations from youngest to oldest are: swamp sediment (2.10 g/cm^3), the Kasai Formation (2.28 g/cm^3), the Muara Enim Formation (2.32 g/cm^3), the Air Benakat Formation (2.39 g/cm^3), the Gumai Formation (2.30 g/cm^3), the Baturaja Formation (2.48 g/cm^3), and lastly the bedrock (2.70 g/cm^3) as the basement.

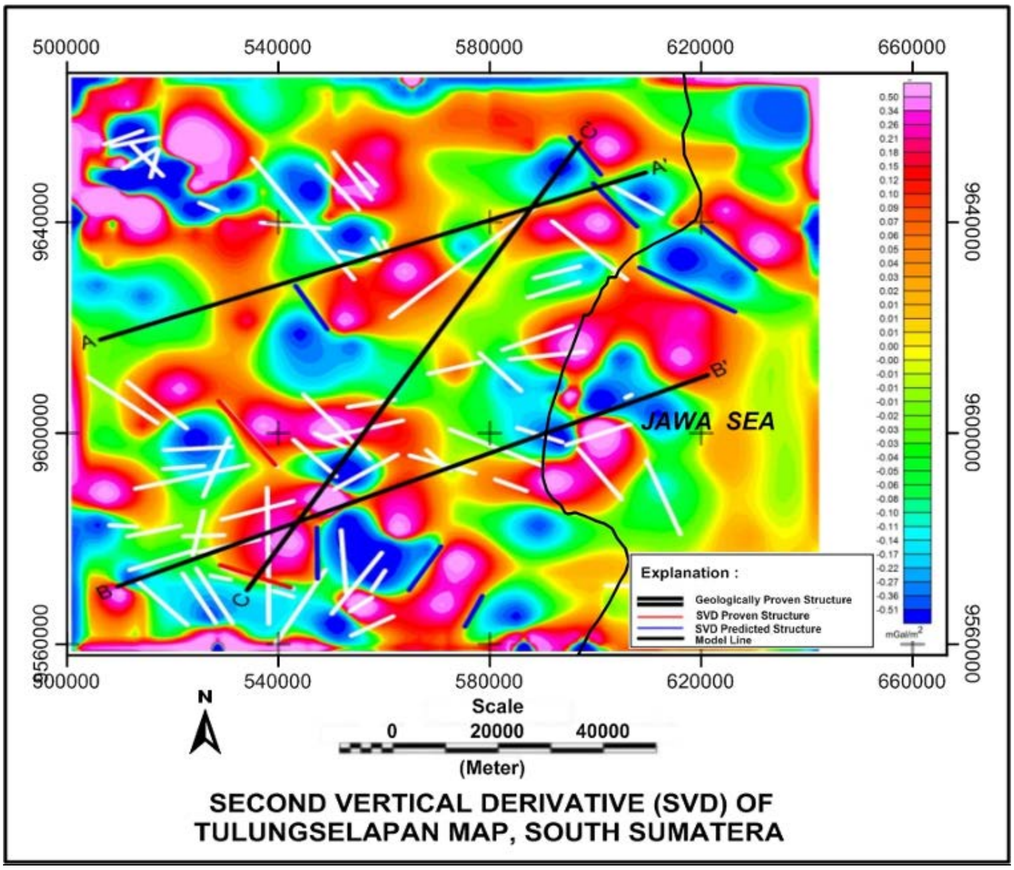

Figure 9. Second Vertical Derivative (SVD) map of Tulung Selapan area, showing faults that indicated geologically or by applying SVD method

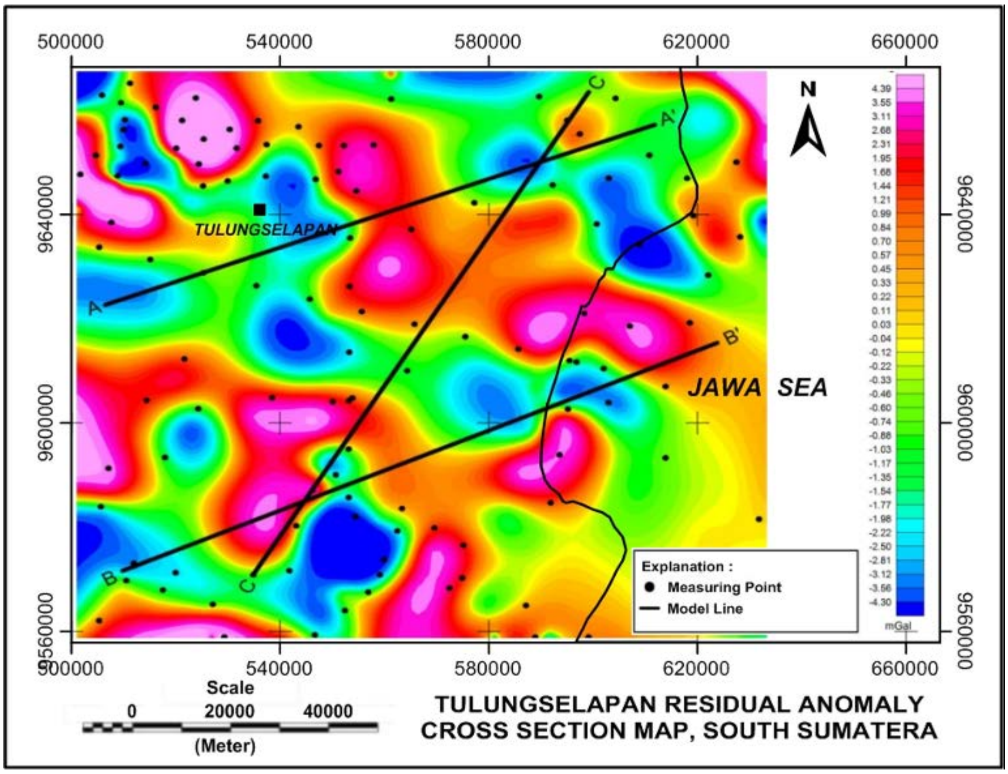

Figure 10. The trajectories (A-A' – B-B' – C-C') used in the 2D forward modeling stage based on residual map of the Tulung Selapan area

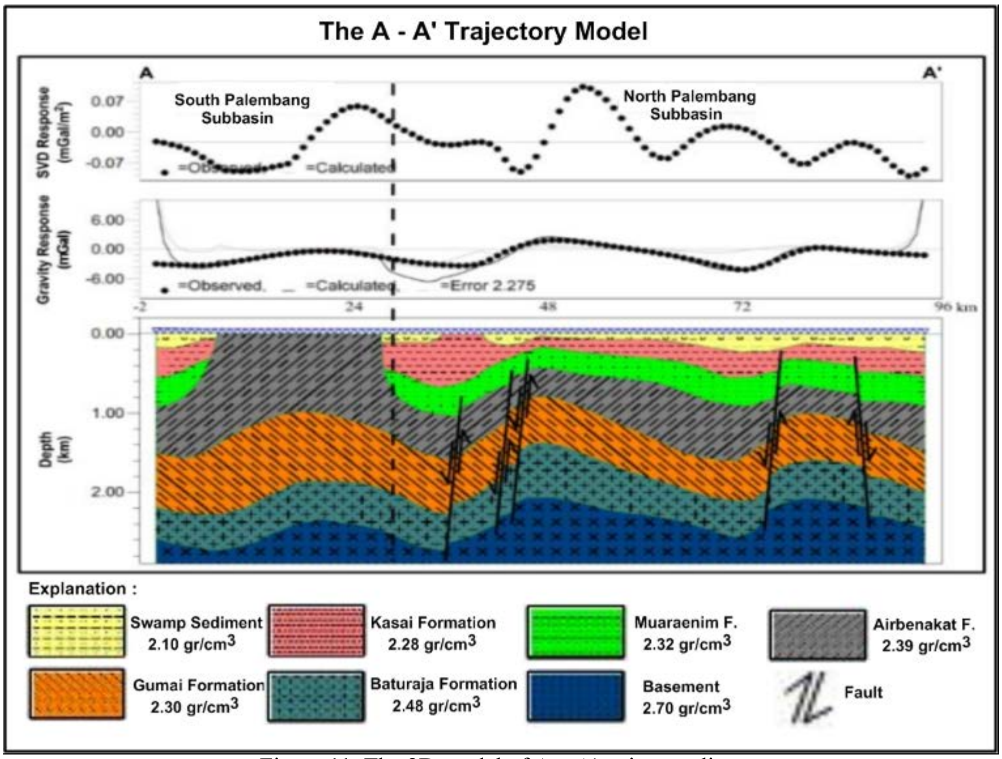

Figure 11. The 2D model of A – A' trajectory line

During the development of the South Palembang and the North Palembang sub-basins in the South Sumatra Basin, the rock formations underwent subduction followed by rifting event in the syn-rift mega-sequence phase, which happened around 40–29 million years ago. The formations also subjected to folding event in the southwest-northeast axis, occurred during the syn-orogenetic mega-sequence phase around 5 million years ago, until the present.

The model did not include the layer overlying the folded formations, assuming it has been eroded. The source rock and reservoir are not able to be identified due to the limited depth of only 2800 m in the modeling. Implicitly, the source rocks and the reservoirs in the South Sumatra Basin are both located in the Talang Akar Formation at a depth of 4000 m below the surface, i.e., the shale rock units and the carbonate rock units, respectively. The caprock in this model is hypothetically the shale of the Gumai Formation at a depth of about 1.53 km and serves as the intraformational seal for trapping hydrocarbons.

The B-B' trajectory (see Figure 10) spans 103 km between the South Palembang sub-basin in the west and the North Palembang sub-basin in the east. The modeling of this trajectory line passes across several faults of northwest-southeast orientation that have already been validated geologically.

The B-B’ trajectory model passes through the South Palembang sub-basin between 0 and 73.5 km. The value of its residual anomaly is moderate to low and shows an increasing and decreasing gravity response. Between 0 and 25.5 km, some deposit units of the Muara Enim Formation are exposed above sea level up to 30 m; then between 46 and 76 km, other deposit units of the Muara Enim Formation are also exposed above sea level up to 40 m. According to the geological map, five normal faults were identified in the South Palembang sub-basin.

The North Palembang sub-basin is traversed between 73.5 and 103 km on the B-B’ trajectory model. Its residual anomalies have low to moderate values, displaying an increasing and decreasing gravity response. Based on the geological map, one normal fault was identified in the North Palembang sub-basin.

Overall, six normal faults are identified across the South and North Palembang sub-basins along the B-B' trajectory line (Figure 12). Resembling the elaboration for the A-A’ trajectory model, the present normal fault structures found in the B-B’ trajectory model were caused by subduction of the Indian-Australian plate, followed by rifting event in the syn-rift mega-sequence phase around 40–29 million years ago, and then folding event in the southwest-northeast direction during the syn-orogenic phase since around 5 million years ago.

In the B-B' trajectory model, the layer above the folded formations is absent, assuming that it has been greatly eroded. The source rock and reservoir also cannot be identified due to the limited depth of the model (only 2800 m below sea level). Like in the A-A’ trajectory model, the source rock is shale rock units of the Talang Akar Formation, while the reservoirs are from its carbonate rock units. The Talang Akar Formation is at a depth of 4000 m below the surface. The caprock is

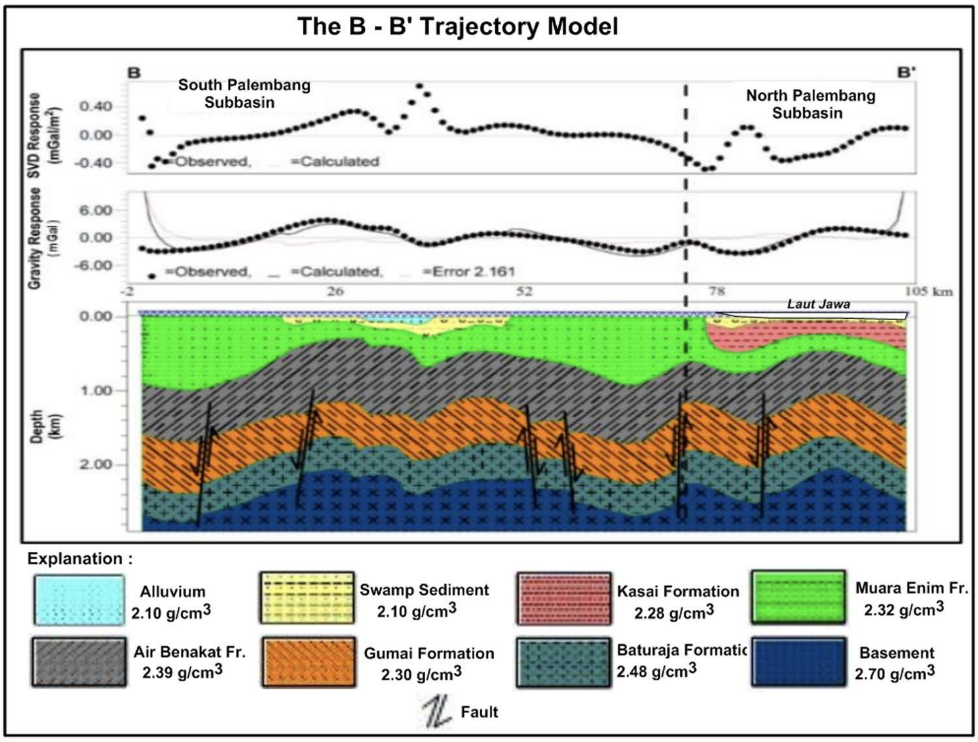

Figure 12. The 2D model of B – B' trajectory line

supposed to be the shale of the Gumai Formation at a depth of about 1.53 km.

Based on the trajectories B - B' from the forward modeling results in Figure 12, there are seven formations of sedimentary rocks and one layer is identified as basement. The youngest age is alluvium (2.10 g/cm^3), successively underlain by swamp deposits (2.10 g/cm^3), the Kasai Formation (2.28 g/cm^3), the Muara Enim Formation (2.32 g/cm^3), the Air Benakat Formation (2.39 g/cm^3), the Gumai Formation (2.30 g/cm^3), until the oldest of the Baturaja Formation (2.48 g/cm^3), and bedrock (2.70 g/cm^3) as the basement.

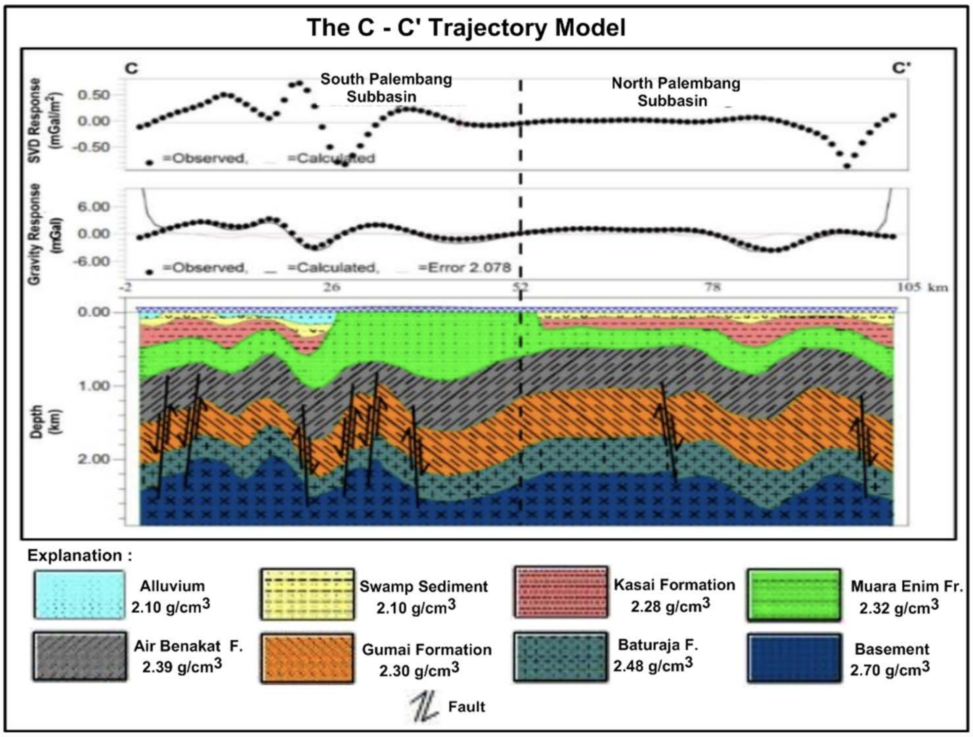

Figure 13. The 2D model of C – C' trajectory line

The C-C' trajectory model (see Figure 10) extends 103 km, perpendicular to several faults of northwest-southeast orientation, which is geologically validated. It passes the South Palembang sub-basin from 0 to 52 km. Here, the values of the residual anomaly are moderate to low, depicting an increasing and decreasing gravity anomaly response. Between 24.5 and 62 km, the Muara Enim Formation deposits are exposed above sea level up to 40 m, or even more. Based on the geological map, six normal faults were identified in this sub-basin.

At a distance between 52 and 102 km, the C-C' trajectory passes through the North Palembang sub-basin, revealing residual anomaly values of moderate to low. Along this distance, gravity anomaly responses are flat, then decline, and finally rise. Based on the geological map, two normal faults were identified in this sub-basin. Overall, eight normal faults were identified along the C-C' trajectory model that formed from the same tectonic events as already elaborated above (Figure 13).

Due to the limited depth of 2800 m, the C–C' trajectory model are not able to identify the source and reservoir rocks. 2D gravity forward modeling identifies seven layers/formations of sedimentary rocks (Figure 13) that from young to old are alluvium (2.10 g/cm^3), swamp sediment (2.10 g/cm^3), the Kasai Formation (2.28 g/cm^3), the Muara Enim Formation (2.32 g/cm^3), the Air Benakat Formation (2.39 g/cm^3), the Gumai Formation (2.30 g/cm^3), and the Baturaja Formation (2.48 g/cm^3); with the bottom layer is interpreted as basement (2.70 g/cm^3).

In accordance with the 2D model and the established South Sumatra Basin petroleum system, the Talang Akar Formation, which is at a depth of about 4 km, is assumed to serve as the source rocks and reservoirs in the Tulung Selapan area, although there is a restraint in the modeling process due to the limited 2800 m depth. The seal rock in this model is expected to be shale rock units of the Gumai Formation (2.30 g/cm^3) which is at an average depth of 1.53 km.

CONCLUSIONS

The pattern of Bouguer gravity anomaly in the study area has a relative northwest-southeast trend of direction and in some places has circular patterns. High anomalies represent rocks with high density (basement rocks), while low anomalies are interpreted as rocks with low density (sedimentary rocks).

The spectral analysis results show that there are two depth boundary planes in the study area, namely the deep and shallow boundary planes. The deep boundary plane (regional) at 17.50 km depth indicates the boundary plane between the upper and lower crust. Thereafter, the shallow boundary plane (residual) at 2.03 km depth indicates the boundary plane between basement and sedimentary rocks. Interpretating the results of SVD gravity data analysis, the fault structure in Tulung Selapan and its surrounding area has a relative northwest-southeast direction.

The 2D modeling from gravity data shows seven layers of sedimentary rocks and bedrock. Sequentially from top to bottom, the uppermost layer is alluvium (2.10 g/cm^3), followed by depositions of swamp sediments (2.10 g/cm^3), the Kasai Formation (2.28 g/cm^3), the Muara Enim Formation (2.32 g/cm^3), the Air Benakat Formation (2.39 g/cm^3), the Gumai Formation (2.30 g/cm^3), the Baturaja Formation (2.48 g/cm^3), and bedrock (2.70 g/cm^3).

ACKNOWLEDGEMENTS

We would like to express our deepest gratitude to the Geological Agency's Head of the Center of Geological Survey (CGS), BRIN's Head of the Research Center for Geological Resources (RCGR), and our lecturers from Institut Teknologi Sumatera, Gestin Mey Ekawati, S.T., M.T. and Rhahmi Adni Pesma, S.Si., M.Si., who assisted with the writing. Appreciation also goes to the team of GRDC (now CGS) that facilitated the field work and provided advice and input for this paper.

REFERENCES

Bishop, M.G., 2000. South Sumatera Basin Province, Indonesia: The Lahat/Talang Akar - Cenozoic total petroleum system. USGS *Open File Report* 99-50S.

Blakely, R.J., 1996. *Potential Theory in Gravity and Magnetic Applications*. Cambridge University Press, 464 pp. ISBN: 9780521575478, 0521575478.

Courteney, S., Cockcroft, P., Lorentz, R., Miller, R., Ott, H.L., Prijosoesilo, P., Suhendan, A.R. and Wight, A.W.R., 1990. *Indonesia - Oil and Gas Fields Atlas, Vol. III: South Sumatera*. Scale not given. Indonesian Petroleum Association Professional Division.

De Coster, G.L., 1974. The geology of the Central and South Sumatera Basins: *Proceedings Indonesian Petroleum Association 3nd Annual Convention*: 77-110.

Elkins, T.A. 1951. The second derivative method of gravity interpretation, *Geophysics*, 16(1): 29-50. DOI: 10.1190/1.1437648.

Grandis, H., 2009. *Pengantar Pemodelan Inversi Geofisika*. Himpunan Ahli Geofisika Indonesia (HAGI), Jakarta, 186 pp. ISBN: 978-979-98933-3-8.

Hutchison, C.S., 1996. *South-East Asian Oil, Gas, Coal and Mineral Deposits*. Oxford Monographs on Geology and Geophysics. Oxford University Press, New York, Oxford. 36: xv + 265 pp.

Karunianto, A.J., Haryanto, D., Hikmatullah, F. and Laesanpura, A., 2017. Penentuan anomali gayaberat regional dan residual menggunakan filter Gaussian, Daerah Mamuju, Sulawesi Barat.

Eksplorium, 38(2):89-98. DOI: 10.17146/eksplorium.2017.38.2.3921.

Mangga, S.A., Sukardi and Sidarto, 1993. *Peta Geologi Lembar Tulung Selapan, Sumatera* (*Geological Map of the Tulung Selapan Quadrangle, Sumatera)*. Scale 1:250,000. Pusat Penelitian dan Pengembangan Geologi.

Panggabean, H. and Santy, L.D., 2012. Sejarah penimbunan Cekungan Sumatera Selatan dan implikasinya terhadap waktu generasi hidrokarbon. *Jurnal Sumber Daya Geologi*, 22(4): 225-235.

Rosid, M.S. and Siregar, H., 2017. Determining fault structure using first horizontal derivative (FHD) and horizontal vertical diagonal maxima (HVDM) method: A comparative study. *AIP Conference Proceedings*, 1862: 030171. DOI: 10.1063/1.4991275.

Reynolds, J.M., 1997. *An introduction to applied and environmental geophysics*. John Wiley, Michigan, 796 pp.

Sekretariat DEN, 2019. *Indonesia Energy Outlook 2019*. Secretariat General of National Energy Council (DEN), Jakarta, 94 pp.

Setiadi, I., Setyanta, B. and Widijono, B.S., 2010. Delineasi cekungan sedimen Sumatra Selatan berdasarkan analisis data gaya berat. *Jurnal Sumber Daya Geologi*, 20(2): 93-106.

Setiadi, I., Diyanti, A. and Nanang, A.D., 2014. Interpretasi struktur geologi bawah permukaan daerah Leuwidamar berdasarkan analisis spektral data gaya berat. *Jurnal Geologi dan Sumberdaya Mineral*. 15(4): 205-214.

Suhendan, A.R., 1984. Middle Neogene depositional environments in Rambutan area, South Sumatra. *Proceedings Indonesian Petroleum Association 13th Annual Convention*: 63-73.

Sosrowidjojo, I.B., Setiardja, B., Zakaria, Kralert, P.G., Alexander, R. and Kagi, R.I., 1994. A new geochemical method for assessing the maturity of petroleum: Application to the South Sumatra basin. *Proceedings Indonesian Petroleum Association 23rd Annual Convention*: 439-455.

Sudarmono, T., Suherman and Eza, B., 1997. Paleogene basin development in Sundaland and it's role to the petroleum systems in Western Indonesia. *Proceedings Indonesian Petroleum Association, International Conference on Petroleum Systems of SE Asia and Australasia*: 545-560.

Tarsis, A.D., 2001. *Penyelidikan batubara bersistim dalam Cekungan Sumatera Selatan di daerah Benakat Minyak dan sekitarnya, Kabupaten Muara Enim Propinsi Sumatera Selatan*. Sub Direktorat Batubara, Direktorat Inventarisasi Mineral, Departemen Energi dan Sumber Daya Mineral, 10 pp.

Wahyudin and Subekti, A.D., 1999. *Pengkajian cekungan gambut di daerah Tulung Selapan, Kabupaten Ogan Komering Ilir, Propinsi Sumatera Selatan*. Pemaparan Hasil Kegiatan Lapangan DIK-S Batubara. Sub Direktorat Eksplorasi Batubara dan Gambut, Direktorat Sumberdaya Mineral, Departemen Pertambangan dan Energi: 10-1–10-3.